




## RESEARCH ARTICLE

# Quantification of SV2A Binding in Rodent Brain Using [<sup>18</sup>F]SynVesT-1 and PET Imaging

Pragalath Sadasivam,<sup>1</sup> Xiaotian T. Fang,<sup>1</sup> Takuya Toyonaga,<sup>1</sup> Supum Lee,<sup>1</sup> Yuping Xu,<sup>1</sup> Ming-Qiang Zheng,<sup>1</sup> Joshua Spurrier,<sup>2</sup> Yiyun Huang,<sup>1</sup> Stephen M. Strittmatter,<sup>2</sup> Richard E. Carson,<sup>1</sup> Zhengxin Cai<sup>1</sup> 

<sup>1</sup>Yale PET Center, Department of Radiology and Biomedical Imaging, Yale University School of Medicine, New Haven, CT, USA

<sup>2</sup>Program in Cellular Neuroscience, Neurodegeneration, and Repair, Departments of Cell Biology, Neurology and Neuroscience, Yale University School of Medicine, New Haven, CT, USA

### Abstract

**Purpose:** Synapse loss is a hallmark of Alzheimer’s disease (AD) and correlates with cognitive decline. The validation of a noninvasive *in vivo* imaging approach to quantify synapse would greatly facilitate our understanding of AD pathogenesis and assist drug developments for AD. As animal models of neurodegenerative and neuropsychiatric disorders play a critical role in the drug discovery and development process, a robust, objective, and translational method for quantifying therapeutic drug efficacy in animal models will facilitate the drug development process. In this study, we tested the quantification reliability of the SV2A PET tracer, [<sup>18</sup>F]SynVesT-1, in a mouse model of AD (APP/PS1) and wild-type controls, and developed a simplified quantification method to facilitate large cohort preclinical imaging studies.

**Procedures:** We generated nondisplaceable binding potential ( $BP_{ND}$ ) and distribution volume ratio (DVR) values using the simplified reference tissue model (SRTM) on the 90-min dynamic PET imaging data, with brain stem and cerebellum as the reference region, respectively. Then, we correlated the standardized uptake value ratio (SUVR)-1 and SUVR averaged from different imaging windows with  $BP_{ND}$  and DVR, using brain stem and cerebellum as the reference region, respectively. We performed homologous competitive binding assay and autoradiographic saturation binding assay using [<sup>18</sup>F]SynVesT-1 to calculate the  $B_{max}$  and  $K_d$ .

**Results:** Using brain stem as the reference region, the averaged SUVR-1 from 30 to 60 min postinjection correlated well with the  $BP_{ND}$  calculated using SRTM. Using cerebellum as the reference region, the averaged SUVR from 30 to 60 min postinjection correlated well with the SRTM DVR. From the homologous competitive binding assay and autoradiographic saturation binding assay, the calculated the  $B_{max}$  and  $K_d$  were 4.5–18 pmol/mg protein and 9.8–19.6 nM, respectively, for rodent brain tissue.

**Conclusions:** This simplified SUVR method provides reasonable SV2A measures in APP/PS1 mice and their littermate controls. Our data indicate that, in lieu of a full 90-min dynamic scan, a 30-min static PET scan (from 30 to 60 min postinjection) would be sufficient to provide quantification data on SV2A expression, equivalent to the data generated from kinetic modeling. The methods developed here are readily applicable to the evaluation of therapeutic effects of novel drugs in this rodent model using [<sup>18</sup>F]SynVesT-1 and small animal PET.

Pragalath Sadasivam and Xiaotian T. Fang contributed equally to this work.

Correspondence to: Zhengxin Cai; e-mail: jason.cai@yale.edu

**Key words:** SV2A, PET, [ $^{18}\text{F}$ ]SynVesT-1, Synapse density, Alzheimer's disease, APP/PS1, SRTM

---

## Introduction

One of the most robust biomarkers of Alzheimer's disease (AD) is the loss of synapses in the hippocampus. As synaptic vesicle glycoprotein 2A (SV2A) is ubiquitously expressed in synaptic vesicles [1], positron emission tomography (PET) imaging of SV2A provides a noninvasive approach to quantify synapse density in living subjects, which can facilitate the drug development for AD, among other neurodegenerative and neuropsychiatric diseases [2–6]. Using the lead SV2A PET tracer, [ $^{11}\text{C}$ ]UCB-J [7], and brain PET imaging, SV2A binding in hippocampus of AD patients at amnesic mild cognitive impairment to mild dementia stage was found to be significantly reduced compared with cognitively unimpaired controls [8, 9]. In addition, the SV2A specific binding in hippocampus correlated with memory test results. Thus, [ $^{11}\text{C}$ ]UCB-J SV2A PET has the potential to distinguish AD patients at an early stage and provide a more objective readout of the pathological progression than conventional cognitive measures. Going from bedside to bench using the same SV2A PET tracer, Toyonaga et al. [10] detected decreased SV2A binding in the hippocampus of a transgenic animal model of AD (APP/PS1 mice), relative to wild type (WT) mice. The decreased SV2A binding was restored to the same level as the WT mice after treatment with a Fyn inhibitor saracatinib, and the effect persisted after stopping the drug treatment. This study demonstrated the proof-of-concept of using preclinical SV2A PET to evaluate therapeutic effects of testing drugs in a mouse model of AD.

Based on [ $^{11}\text{C}$ ]UCB-J, we have designed, synthesized, and translated to human studies two novel  $^{18}\text{F}$ -labeled SV2A PET radiotracers, [ $^{18}\text{F}$ ]SynVesT-1, and [ $^{18}\text{F}$ ]SynVesT-2, both of which demonstrated unique pharmacokinetic profiles in nonhuman primate and human brains [11–13]. As preclinical research using rodent models of neurodegenerative and neuropsychiatric diseases is critical in our understanding of these diseases and development of novel therapeutics, the objective of this study is to (1) assess the pharmacokinetics and quantification methodologies of [ $^{18}\text{F}$ ]SynVesT-1 in rodent brain PET; (2) simplify the quantification method for large cohort animal imaging studies in evaluating experimental AD drug treatment effects; (3) estimate the  $B_{\text{max}}$  and  $K_{\text{d}}$  of [ $^{18}\text{F}$ ]SynVesT-1 in rodent brain tissue.

## Materials and Methods

### Radiochemistry

(*R*)-4-(3-Fluoro-5-(fluoro- $^{18}\text{F}$ )phenyl)-1-((3-methylpyridin-4-yl)methyl)pyrrolidin-2-one ([ $^{18}\text{F}$ ]SynVesT-1) was

synthesized from the corresponding organotin precursor following previously published procedure [12]. Briefly,  $^{18}\text{F}$ -fluoride was produced via the  $^{18}\text{O}(\text{p}, \text{n})^{18}\text{F}$  nuclear reaction in a GE PETtrace cyclotron (Uppsala, Sweden) and delivered as an aqueous  $^{18}\text{F}$ -fluoride solution in  $^{18}\text{O}$ -water. The  $^{18}\text{F}$ -fluoride anion was trapped on a pre-activated anionic exchange resin cartridge (Chromafix-PS- $\text{HCO}_3$ ), then eluted from the cartridge with a solution containing KOTf and  $\text{K}_2\text{CO}_3$ , and dried azeotropically under argon at 110 °C. Further drying was achieved using MeCN at 110 °C. A solution containing the tin precursor, (*R*)-4-(3-fluoro-5-(trimethylstannyl)phenyl)-1-((3-methylpyridin-4-yl)methyl)pyrrolidine-2-one (2 mg) in anhydrous dimethylacetamide (DMA) was added to the dried  $^{18}\text{F}$ , followed by a solution containing pyridine, DMA and copper(II) triflate, which was then heated at 110 °C for 20 min. The reaction mixture was purified under semipreparative HPLC conditions (Luna C18(2) column), eluting with a mobile phase containing  $\text{CH}_3\text{CN}$ , 0.1 M ammonium formate and AcOH (pH 4.2) at a flow rate of 5 mL/min. The product was collected into DI water and then trapped on a Waters C18 SepPak cartridge. The cartridge containing the product was washed with dilute HCl solution (0.001 N). The trapped product was recovered by elution with U.S. Pharmacopeial Convention (USP) EtOH followed by USP saline. The resulting mixture was then passed through a sterile membrane filter (0.22  $\mu\text{m}$ , Merck Millipore, Ireland) for sterilization and collected in a sterile vial precharged with saline and  $\text{NaHCO}_3$  USP solution to afford a formulated solution ready for administration.

Chemical purity, radiochemical purity, and molar activity were determined by HPLC analysis of the final product solution. Identity of the labeled compound was confirmed by co-injection of the product with the reference standard of SynVesT-1.

### Homologous Binding Assay

The homologous binding assay was carried out using [ $^{18}\text{F}$ ]SynVesT-1 as the radioligand, unlabeled SynVesT-1 standard as blocking agent, and mouse brain homogenate in 96-well plates (PerkinElmer, MA, USA). Briefly, mouse brain homogenate was prepared and stored as homogenate solutions (100 mg/mL). The homogenate solution was diluted with binding buffer (2 mM  $\text{MgCl}_2$  in 50 mM Tris HCl, pH 7.4) to a final concentration of 0.01 mg protein in 140  $\mu\text{L}$  solution for each sample well. An aliquot of 20  $\mu\text{L}$  of a series of SynVesT-1 standard solutions with increasing concentrations (0.1, 0.3, 1, 3, 10, 30, 60, 100, 300, 1000,

50,000 nM) was added to each sample well. Then, aliquots of 20  $\mu\text{L}$  of [ $^{18}\text{F}$ ]SynVesT-1 ( $\sim 0.074$  MBq, 2.3 nM) and appropriate amounts of binding buffer were added to each sample to reach the final volume of 200  $\mu\text{L}$  per sample. The 96-well plate was incubated on a Thermoshaker at 37  $^{\circ}\text{C}$  for 30 min. After incubation, the plate was washed twice with 200  $\mu\text{L}$  of binding buffer and the filters were harvested and counted using a gamma counter. Because the hot and cold ligands have identical affinities, i.e.,  $K_d$  and  $K_i$  are identical, we fitted the specific binding data nonlinearly to estimate the  $\text{IC}_{50}$  of SynVesT-1 and calculate the  $K_d$  and  $B_{\text{max}}$  using the following equations:

$$K_d = K_i = \text{IC}_{50} - [\text{radioligand}]$$

$$B_{\text{max}} = (\text{total binding} - \text{nonspecific binding}) / ([\text{radioligand}] / (K_d + [\text{radioligand}]))$$

Total binding is determined by the bound radioligand normalized by protein weight (pmol/mg) from samples without the added unlabeled SynVesT-1 standard, representing the combined specific binding and nonspecific binding signal at the radioligand concentration ( $[\text{radioligand}]$ ). Nonspecific binding is determined by blocking the specific binding with excess amount of the unlabeled SynVesT-1 standard (0.05 mM).

### Autoradiography Saturation Binding

Brain tissue from WT mice (female, 69.3  $\pm$  4.7 weeks) were sagittally sectioned using a cryostat at 20 micron (Leica CM1850), mounted onto Superfrost<sup>TM</sup> Plus slides (Thermo Fisher Scientific, Waltham, MA) and stored at  $-80^{\circ}\text{C}$  until further use. On the day of the experiment, sections were thawed for 25 min, rehydrated in ice-cold phosphate buffered saline (PBS, pH 7.4) for 5 min, then incubated for 1 h at room temperature with the following concentrations of [ $^{18}\text{F}$ ]SynVesT-1: 100 nM, 50 nM, 25 nM, 10 nM, 5 nM, 2.5 nM, and 1.0 nM in PBS, and adjacent sections were incubated with the same concentration range of [ $^{18}\text{F}$ ]SynVesT-1 containing 1 mM levetiracetam (an SV2A-specific ligand). Brain sections were washed in ice-cold PBS ( $3 \times 5$  min), briefly dipped in D.I. water and dried in a fume hood for 1 h. A calibration standard, with eight dilutions, was prepared in duplicate from a starting [ $^{18}\text{F}$ ]SynVesT-1 activity of 1.0 MBq  $\text{mL}^{-1}$ . Air-dried sections along with the calibration standard were exposed to a BAS SR 2040 imaging plate ( $20 \times 40$  cm, Fujifilm, Japan) for 18 h. The plate was scanned with a Typhoon Phosphor Trio imaging system. Image analysis and quantification were carried out using Fiji (ImageJ, NIH).

### Animals

Mice were cared for by the Yale Animal Resource Center, and all animal experiments were approved by Yale's Institutional Animal Care and Use Committee. Wildtype (WT) mice (C57BL/6J) and APP/PS1 mice (female, 88  $\pm$  4 weeks) [14]

were purchased from Jackson Laboratory and maintained on a C57BL/6J background as described previously [15–17]. As the group comparison is out of the scope of this study, we chose to use a single sex in this study.

### PET Imaging Experiments

The SV2A PET tracer [ $^{18}\text{F}$ ]SynVesT-1 was administered intravenously via lateral tail vein as a bolus ( $10.28 \pm 3.74$  MBq, in 0.1 mL) to 3 APP/PS1 mice and 3 WT mice under anesthesia. Animals were kept under 1.5–2.5 % isoflurane on a heating pad for the duration of the entire scan. They underwent baseline PET scans. Emission data were acquired from 0 to 90 min post-injection (*p.i.*) on an Inveon small animal PET/CT scanner (Siemens Medical Solutions, Knoxville, TN, USA). Images were reconstructed with 3D ordered subset expectation maximization method (OSEM3D; 2 iterations, 16 subsets) with maximum *a posteriori* probability algorithm (MAP; 25 iterations) with corrections for decay, attenuation, scatter, normalization, and randoms.

### Image Analysis

An averaged PET image from 0 to 90 min for each measurement (mean of all frames) was coregistered to a representative PET image of [ $^{11}\text{C}$ ]UCB-J resliced in Ma-Benveniste-Mirrione mouse brain atlas template space. Registration was performed with a 6 degree-of-freedom linear registration using FMRIB's Linear Image Registration Tool in FSL. ROIs were extracted from the atlas and regional time-activity curves (TACs) were obtained by applying template ROIs to the PET images. Analysis included the following ROIs: amygdala, basal forebrain septum, brain stem (BS), brain stem with cerebellum, cerebellum (CB), cingulate cortex, cortex, hippocampus, hypothalamus, inferior colliculi, mid brain, striatum, superior colliculi, thalamus, and whole brain.

### Quantitative Analysis

The simplified reference tissue model (SRTM) [18] was used to estimate nondisplaceable binding potential ( $BP_{\text{ND}}$ ) using BS as the reference region and to estimate distribution volume ratio (DVR) using CB as a reference region. Additionally, DVRs were estimated using the Logan graphical analysis with a reference region input function and 2 parameters as described in Eq. 7 by Logan and colleagues using  $t^*$  values of 0, 10, 20, and 30 min [19]. Standardized uptake values (SUVs) of brain regions averaged from 20 to 50 min, 30 to 60 min, 40 to 70 min, 50 to 80 min, and 60 to 90 min *p.i.* were normalized with BS to generate SUV ratio (SUVR) as  $\text{SUVR-1}_{(\text{BS})}$  and also normalized with CB to generate  $\text{SUVR}_{(\text{CB})}$ .  $\text{SUVR-1}_{(\text{BS})}$  and  $\text{SUVR}_{(\text{CB})}$  values from different time windows were correlated with  $BP_{\text{ND}}$  and DVR values to determine the optimal static imaging window.

## Results

### Radiochemistry

The SV2A PET tracer [ $^{18}\text{F}$ ]SynVesT-1 was synthesized using its trimethyl tin precursor following published procedures [12]. The radiochemical purity was  $> 99\%$ . The molar activity was  $264 \pm 90$  MBq/nmol ( $n = 3$ ). Total synthesis time including purification and formulation for [ $^{18}\text{F}$ ]SynVesT-1 was around 90 min.

### Homologous Competitive Binding Assay Using Rodent Brain Homogenate to Determine $B_{\max}$ and $K_d$

In order to determine specific [ $^{18}\text{F}$ ]SynVesT-1 binding to mouse brain, a homologous competitive binding assay was performed using mouse brain homogenate. The calculated  $K_d$  was  $19.6 \pm 1.38$  nM, with  $B_{\max}$  of 4.54 pmol/mg protein (Fig. 1a), which is lower than the  $B_{\max}$  of mouse forebrain homogenate reported by Kaminski et al. (8.8 pmol/mg) [20], and higher than the  $B_{\max}$  of mouse brain membrane reported by Gillard et al. (1.5 pmol/mg) [21]. This is probably due to different assay conditions used at different labs.

### Binding Assay Using Autoradiography to Determine $B_{\max}$ and $K_d$

Alternatively, a saturation binding assay was performed using mouse brain sections and autoradiography method (Figure S1). Coincubation with levetiracetam (1 mM) reduced total binding signal to nonspecific levels. The nonspecific binding increased linearly with tracer concentration. Total binding appeared to saturate at radioligand concentrations above 25 nM. Using this autoradiographic method, the  $B_{\max}$  was determined to be  $1.8 \pm 0.1$  pmol/mg of brain tissue or  $18 \pm 1$  pmol/mg protein, assuming 10 % of brain tissue is protein.  $K_d$  was calculated to be  $9.8 \pm 1.7$  nM (Fig. 1b).

These measured  $K_d$  values of SynVesT-1 (9.8–19.6 nM) in mouse brain homogenate or sections are higher than the  $K_d$  of UCB-J in rat brain homogenate ( $K_d = 2.6 \pm 0.25$  nM;  $B_{\max} = 0.81 \pm 0.025$  pmol/mg protein) and the  $K_i$  of SynVesT-1 (2.2 nM) measured using [ $^3\text{H}$ ]UCB-J and competitive binding assay in rat whole brain [22].

### Rodent PET Imaging and Data Analysis

Representative SUV<sub>30-60 min</sub> images of the WT and APP/PS1 mice are shown in Fig. 2a. SUV values were generally higher in WT brain than in APP/PS1 brain. TACs generated from dynamic scans are shown with three highlighted brain regions (hippocampus, brainstem and cerebellum) in Fig. 3. TACs demonstrated rapid tracer entrance into the brain, peaking within 20 min *p.i.*, followed by steady washout,

indicating efficient BBB penetration and reversible binding kinetics in rodent brain. For all mice, brainstem demonstrated the lowest SUV, while superior colliculi had the highest peak SUV, consistent with the SV2A expression pattern mapped with [ $^3\text{H}$ ]UCB-J autoradiography in rodent brains [22]. In comparison to [ $^{11}\text{C}$ ]UCB-J in the same rodent models [10], [ $^{18}\text{F}$ ]SynVesT-1 image analysis relied on BS and CB as reference region for this study.

First, to assess if the single tissue compartment assumption requirement of SRTM is valid, we estimated DVRs with Logan graphical analysis. We found that the Logan reference plots are linear throughout the imaging time for  $t^*$  (0, 10, 20, 30 min) using either brainstem (Figure S2a) or cerebellum as reference region (Figure S2b). As well, Logan reference DVRs estimated with  $t^* = 0$  min correlated well with DVRs estimated with  $t^* = 10$  min (Figure S2c) for both brainstem (blue,  $Y = 1.004 * X - 0.03822$ ,  $R^2 = 0.9983$ ) and cerebellum (red,  $Y = 1.004 * X - 0.02169$ ,  $R^2 = 0.9969$ ) as reference region. As such, we determined that  $t^*$  of 0 min was valid and subsequent comparisons were made against Logan reference DVRs estimated with  $t^* = 0$  min.

Next, we applied SRTM to this data set and found that  $BP_{\text{ND}}$  and DVR values were estimated reliably with low fitting errors (standard errors  $< 5\%$  for all ROIs) using BS and CB as reference region, respectively (Fig. 2b). Logan reference DVR correlated well with SRTM-derived DVR (Figure S1d) for both brainstem (blue,  $Y = 1.012 * X - 0.06149$ ,  $R^2 = 0.9852$ ) and cerebellum (red,  $Y = 0.9976 * X - 0.0242$ ,  $R^2 = 0.9808$ ) as reference. These results suggest that the single tissue compartment assumption is valid, as well as support the use of SRTM.

To increase the throughput of PET scanning and simplify the quantification workflow, we compared the averaged SUVR-1<sub>(BS)</sub> from different imaging windows with  $BP_{\text{ND}}$  calculated using the complete data sets to identify a suitable static imaging window for [ $^{18}\text{F}$ ]SynVesT-1 in mice. Comparisons of SRTM  $BP_{\text{ND}}$  with SUVR-1<sub>(BS)</sub> calculated using 30 min time intervals (from 20 to 50 min, 30 to 60 min, 40 to 70 min, 50 to 80 min, and 60 to 90 min) across all brain ROIs are shown in Fig. 4. The SUVR-1<sub>(BS)</sub> at all time intervals correlated with  $BP_{\text{ND}}$  values well for all brain regions ( $R^2 = 0.9601, 0.9523, 0.9372, 0.9167, \text{ and } 0.8945$  for data from 20 to 50 min, 30 to 60 min, 40 to 70 min, 50 to 80 min, and 60 to 90 min, respectively).  $BP_{\text{ND}}$  and SUVR-1<sub>(BS)</sub> using scan data from 20 to 50 min *p.i.* had the highest correlation, which overlaps with line of identity for all ROIs (Fig. 4a,  $Y = 1.053X + 0.00393$ ,  $R^2 = 0.9601$ ,  $p < 0.0001$ ); while scan data from 30 to 60 min *p.i.* showed the best linearity for hippocampus (Fig. 4b,  $Y = 0.867X - 0.1831$ ,  $R^2 = 0.7961$ ,  $p = 0.0564$ ). The  $BP_{\text{ND}}$  and SUVR-1<sub>(BS)</sub> agreement deteriorated at later time windows (as assessed by Pearson correlation coefficient for all ROIs) compared to the 20–50 min and 30–60 min imaging windows. The SUVR-1<sub>(BS)</sub> from later time windows appeared to overestimate  $BP_{\text{ND}}$  and the fitted lines shifted from the line of identity to a larger extent, with increasing y-intercepts (Fig.



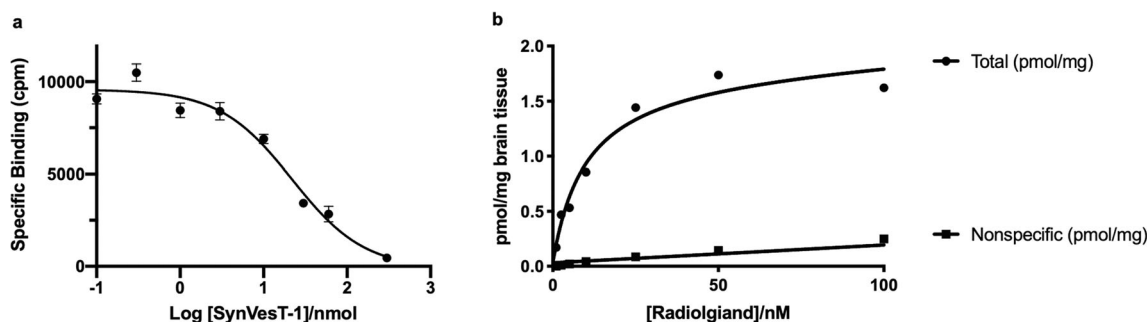


**Fig. 1** [ $^{18}\text{F}$ ]SynVesT-1 *in vitro* binding assay results. **a** Specific-binding signal (i.e., nonspecific subtracted from total) against the logarithm of total concentration of SynVesT-1 (both hot and cold ligand in nM) from homologous competitive binding assay using rodent brain homogenate; **b** Total and nonspecific binding determined by blocking with levetiracetam (1 mM) from autoradiography saturation binding assay using rodent brain sections.

4c–e). Therefore, the 20–50 min and 30–60 min time windows were identified as suitable static imaging windows to allow for the shortening of PET scan time; this increases the maximum number of animals we are able to scan per tracer synthesis (see the “Discussion” section for the theoretical calculation of the maximum number of mice that can potentially be scanned using the optimized imaging protocol).

As the cerebellum is affected the least throughout AD progression, it could potentially be used as a reference region in AD patients and the APP/PS1 mouse model as well. We performed linear correlation analysis of  $\text{DVR}_{(\text{CB})}$  from 90 min of PET data and  $\text{SUVR}_{(\text{CB})}$  calculated from 30-min intervals across all brain regions.  $\text{DVR}_{(\text{CB})}$  and  $\text{SUVR}_{(\text{CB})}$  demonstrated excellent agreement for all ROIs within all the time intervals ( $R^2 > 0.95$ ). For example, data from the 30–60 min window interval showed excellent correlation between  $\text{DVR}_{(\text{CB})}$  and  $\text{SUVR}_{(\text{CB})}$  for all brain regions ( $Y = 1.035X - 0.0157$ ,  $R^2 = 0.982$ ,  $p < 0.0001$ ) and

the hippocampus ( $Y = 0.8274X + 0.2899$ ,  $R^2 = 0.8422$ ,  $p = 0.0099$ ), as well as all other time intervals, up to 90 min (Fig. 5). Using cerebellum as reference region,  $\text{SUVR}$  (30–60 min) also correlated well with Logan DVR ( $Y = 0.9838 * X + 0.06765$ ,  $R^2 = 0.9713$ , Figure S1e).

## Discussion

Unlike traditional research methods using electron microscopy (EM), immunohistochemistry (IHC), or Western blot analysis for quantification of synapses or synaptic proteins, *in vivo* synapse quantification using PET imaging requires small molecule ligands that specifically target synaptic proteins. Among the commonly used biomarkers for synapse, e.g., synaptophysin, synaptotagmin, synaptosomal-associated protein, 25 kDa (SNAP-25), etc., SV2A stands out as it has brain penetrant small molecule ligands such as levetiracetam (Keppra) [23], making SV2A a feasible target for brain PET imaging. A medicinal chemistry study around this pharmacophore led to the

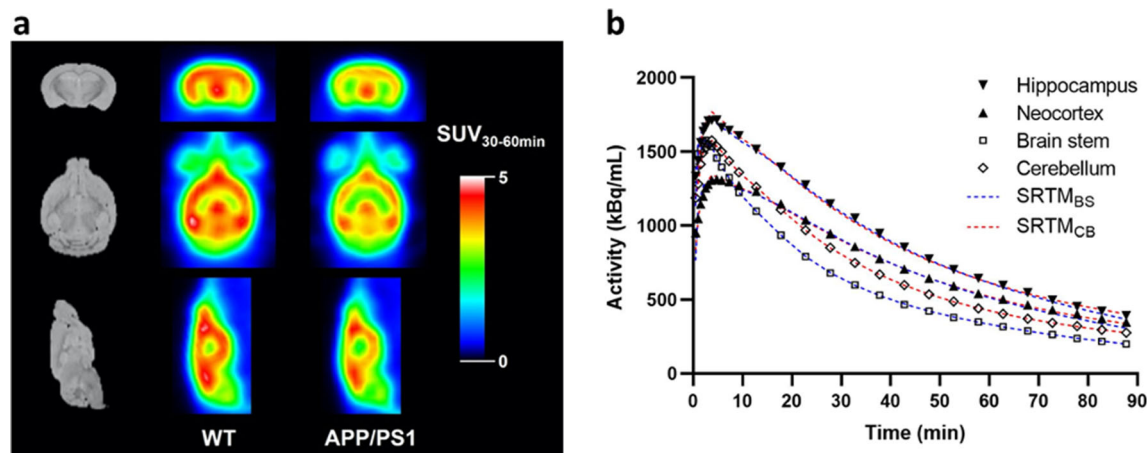


**Fig. 2** **a** Representative summed coronal (top row), axial (middle row), and sagittal (bottom row) SUV images of [ $^{18}\text{F}$ ]SynVesT-1 from 30 to 60 min in WT (middle column) and APP/PS1 mouse brains (right column), with anatomical MR images in Ma-Benveniste-Mirrione mouse brain atlas (left column) as anatomical reference. **b** Time-activity curves of regional brain radioactivity in hippocampus, neocortex, brain stem (BS) and cerebellum (CB). Dotted lines show curve fitting with SRTM using either BS (blue) or CB (red) as reference region.

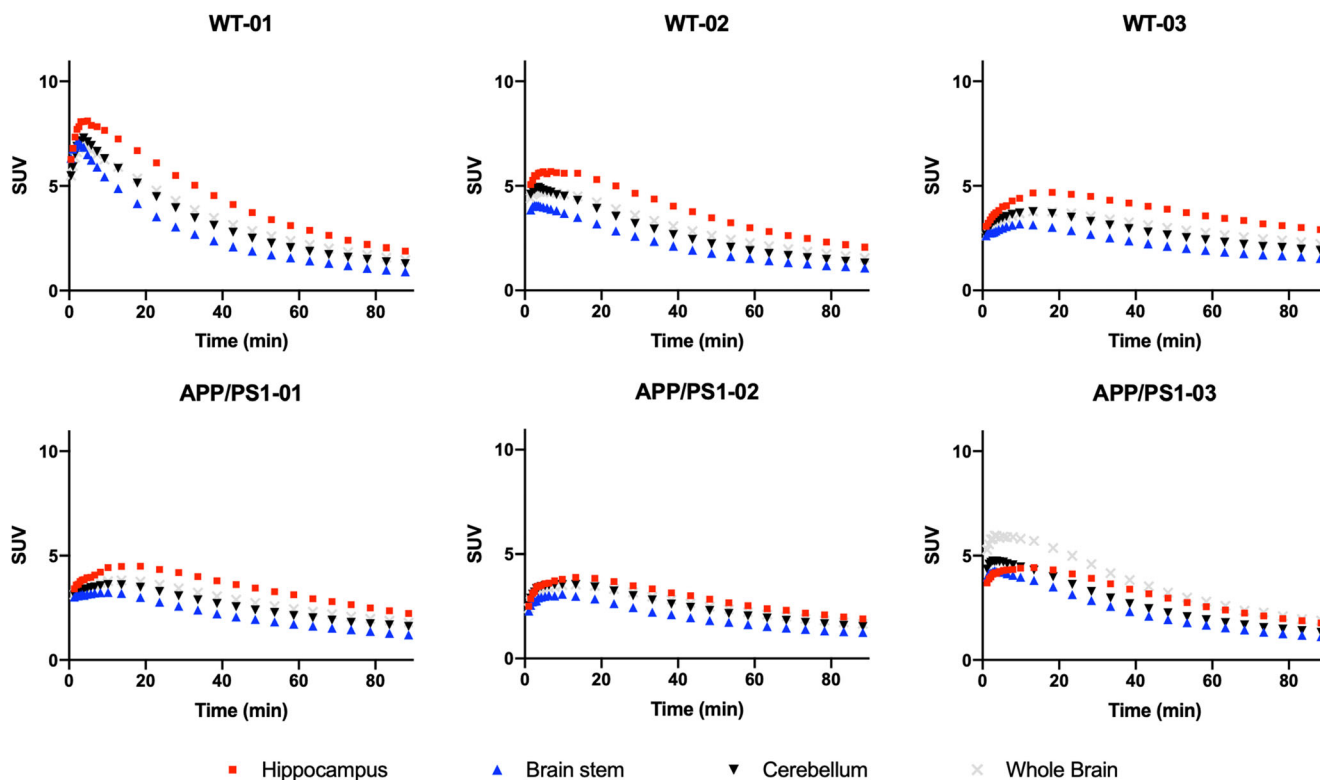


Fig. 3 Time activity curves of selected brain regions from 0 to 90 min postinjection (*p.i.*) of [ $^{18}\text{F}$ ]SynVesT-1 in wild type mice (WT, top row) and APP/PS1 mice (bottom row). Hippocampus (red), brainstem (blue), cerebellum (black), and whole brain (grey).

discovery of SV2A ligands with nanomolar  $IC_{50}$  and improved physicochemical properties for brain PET imaging [24]. From this library of SV2A ligands, the first generation SV2A PET imaging probes were developed, *i.e.*, [ $^{11}\text{C}$ ]UCB-A [25], [ $^{18}\text{F}$ ]UCB-H [26], and [ $^{11}\text{C}$ ]UCB-J [7]. The discovery of these SV2A PET ligands enabled PET imaging of SV2A, a noninvasive approach to quantify synapse density in living subjects, and has boosted our insight to the pathogenesis and pathophysiology of neurodegenerative and psychiatric diseases [2]. At the Yale PET Center, SV2A PET with [ $^{11}\text{C}$ ]UCB-J has been applied in a variety of neurodegenerative and psychiatric disorders, *i.e.*, AD [8, 9], Parkinson's disease [6], epilepsy [4], schizophrenia [5], and depression [3], with many ongoing clinical studies.

Based on the lead SV2A PET tracer, [ $^{11}\text{C}$ ]UCB-J [4, 7], we further developed two novel  $^{18}\text{F}$ -labeled SV2A radiotracers, [ $^{18}\text{F}$ ]SynVesT-1, and [ $^{18}\text{F}$ ]SynVesT-2, for SV2A PET imaging and demonstrated their unique pharmacokinetics profiles in nonhuman primates [11, 12]. With a longer half-life, the fluorine-18-labeled SV2A PET tracers will allow for central production and distribution to PET centers for multicenter clinical trials and routine clinical use. They will also benefit preclinical studies by allowing more animals to be scanned using a single dose of radiotracer. Based on our homogenate binding assay results and the assumption that the cerebral protein content is 10 % and rodent cerebral density is 1 g/mL, the  $B_{\text{max}}$  of SV2A in mouse brain is 454 nM. In order to occupy less than 5 % of SV2A, a maximum of 11.35 pmol of cold

SynVesT-2 is allowed to bind specifically in the brain. Assuming the average whole brain SUV is 5 and the brain occupies 2 % of the body weight of the rodent (25 g), a total of 10 % of the injected drug will be taken into brain. Thus, a single injection dose of 1.85 MBq requires a minimum molar activity of 16.3 MBq/nmol for [ $^{18}\text{F}$ ]SynVesT-1 to guarantee less than 5 % of SV2A to be occupied by the injected ligand, even with negligible nonspecific brain uptake. This means a typical dose of [ $^{18}\text{F}$ ]SynVesT-1 is usable for rodent PET scan even after 6 h posttracer synthesis, as the typical molar activity of [ $^{18}\text{F}$ ]SynVesT-1 (264 MBq/nmol at end of synthesis) is 27.2 MBq/nmol at 6 h postsynthesis, which is still greater than the minimally required molar activity (16.3 MBq/nmol). It is noteworthy that another limiting factor for the maximum number of animals to be scanned is the concentration of [ $^{18}\text{F}$ ]SynVesT-1 in the dose vial. Using the maximum injection volume of 0.1 mL and minimum injection activity of 1.85 MBq per mouse, to allow for injections at 6 h postsynthesis, the minimum amount of [ $^{18}\text{F}$ ]SynVesT-1 in a 10 mL dose is 1796 MBq, which is readily achievable based on the current radiochemical yields.

Modern translational neuropharmacological research relies on animal models of human CNS diseases to identify or validate disease pathways and therapeutic targets as well as to evaluate potential therapeutics [27, 28]. Thus, we set out to assess the pharmacokinetics and quantification methods using [ $^{18}\text{F}$ ]SynVesT-1 in rodent PET imaging and simplified the quantification method to allow for more efficient large cohort animal imaging studies.

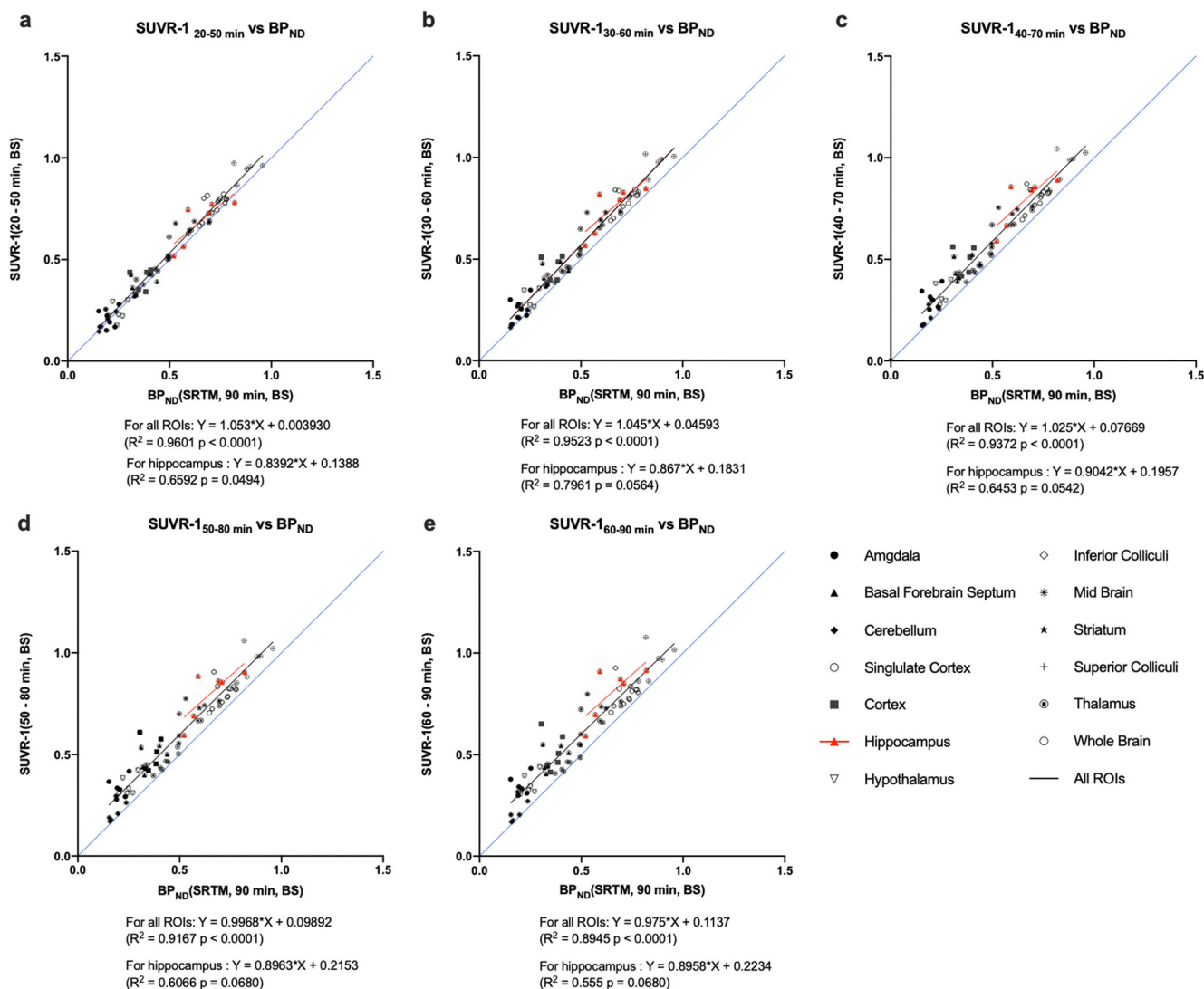


**Fig. 4** Linear correlation analysis of SUVR (region-to-brain stem) -1 using data from scan time **a** 20–50 min, **b** 30–60 min, **c** 40–70 min, **d** 50–80 min, and **e** 60–90 min with  $BP_{ND}$  values calculated through SRTM using the full 90-min scan time and brain stem (BS) as reference region. Hippocampus values shown in red.

In a recent kinetic modeling study of [ $^{11}\text{C}$ ]UCB-J PET in mice, Berbglio *et al.* tested different kinetic models using image-derived input function (IDIF) with or without metabolism corrections and found that 1TCM is the preferred model for reliable estimation of  $V_T$  values and at least 60-min dynamic scan is needed for each mouse using [ $^{11}\text{C}$ ]UCB-J [29]. But the short decay half-life of carbon-11 ( $\sim 20$  min) and the requirement of 60-min dynamic scan limits the imaging throughput and full kinetic modeling requires a nontrivially obtained input function.

Alternatively, the ratio of SUVs of brain regions to a reference region at equilibrium can be used to estimate specific binding in the target brain regions [30]. For clinical [4, 9] and preclinical [7, 12, 31, 32] SV2A PET imaging studies, the white matter region (centrum semiovale) has been used as the reference region. Although minimal SV2A protein was detected by western blotting in centrum

semiovale, the SV2A PET signal in centrum semiovale could be partially blocked in humans by levetiracetam even after minimizing or correcting partial volume effects, indicating SV2A specific uptake in centrum semiovale [33]. As the white matter is too small to be used as reference region in rodent brain PET, other brain regions which are less impacted by disease processes are needed to normalize the PET imaging data. In a previous study using [ $^{11}\text{C}$ ]UCB-J in the same rodent model (APP/PS1 mouse model of AD and C57BL/6J littermate control), brain stem was used as the reference region to calculate  $SUVR-1_{(BS)}$  as a surrogate for  $BP_{ND}$  [10]. In that study, the averaged  $SUVR-1_{(BS)}$  from 30 to 60 min *p.i.* correlated well with  $BP_{ND}$  calculated using SRTM ( $Y = 1.03X + 0.02$ ,  $R^2 = 0.86$ ,  $p < 0.0001$ ) for all brain ROIs. In this study using [ $^{18}\text{F}$ ]SynVesT-1, the  $SUVR-1_{(BS)}$  (30–60 min *p.i.*) and  $BP_{ND}$  also demonstrated excellent correlation within all ROIs ( $Y = 1.045X + 0.04593$ ,  $R^2 =$

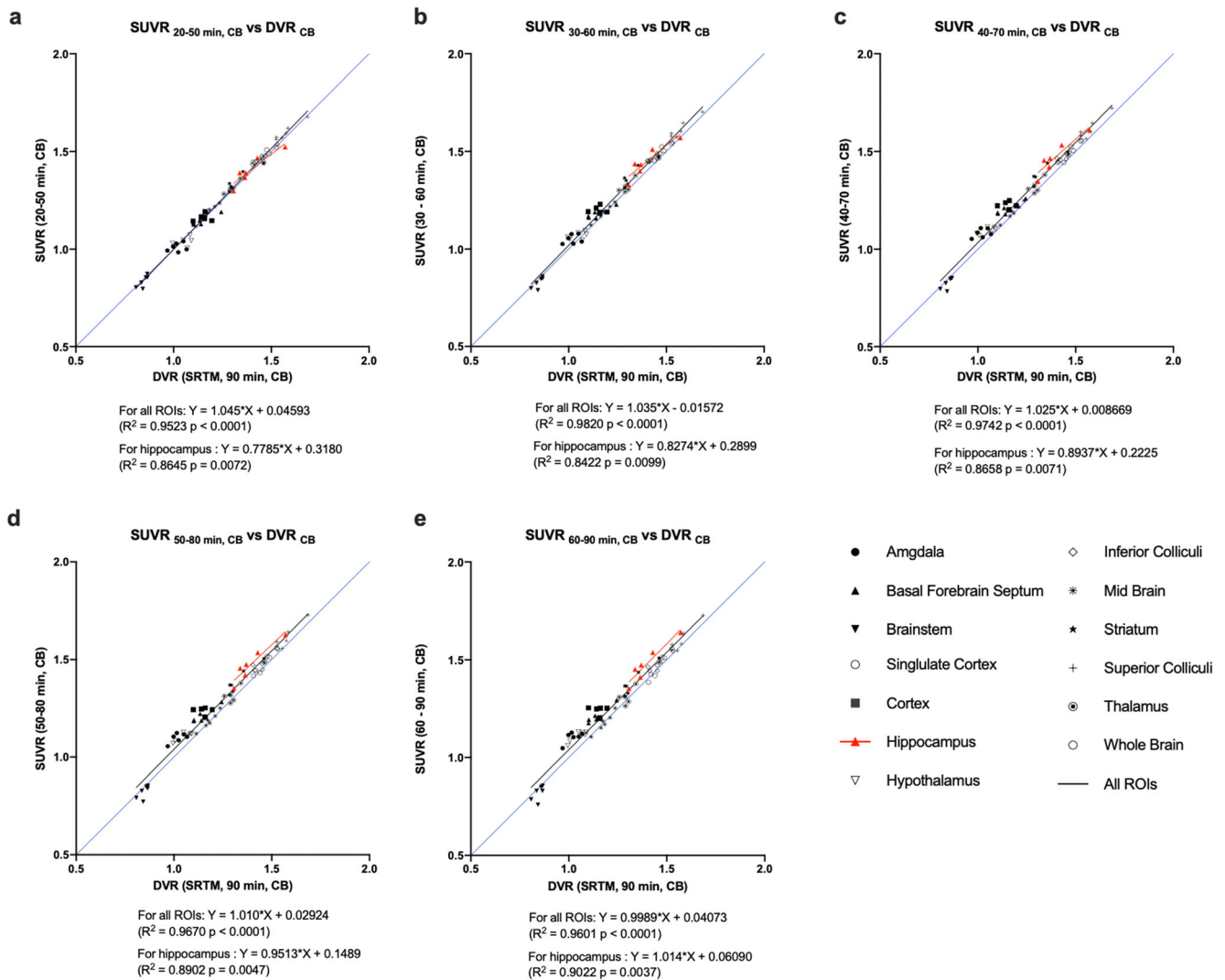


**Fig. 5** Linear correlation analysis of SUVR (region-to-cerebellum) using data from scan time **a** 20–50 min, **b** 30–60 min, **c** 40–70 min, **d** 50–80 min, and **e** 60–90 min with DVR values estimated with SRTM using the full 90-min scan time and cerebellum (CB) as reference region.

0.95,  $p < 0.0001$ ), using [ $^{18}\text{F}$ ]SynVesT-1 (Fig. 4b). Thus, the same optimal imaging window (30–60 min *p.i.*) can be used for mouse brain SV2A PET quantification using either [ $^{11}\text{C}$ ]UCB-J or [ $^{18}\text{F}$ ]SynVesT-1. This indicated similar pharmacokinetics of these two PET tracers in mice, consistent with the findings in nonhuman primates [7, 12] and humans [4]. In the previous study using [ $^{11}\text{C}$ ]UCB-J in the same animal model, when brain stem was used as the reference region, we found increased variability because of the small size of the brain stem. To reduce the variability, whole brain was used as an alternative solution for normalization, which provided more consistent results but with significantly reduced magnitude of group difference (WT vs APP/PS1). In this study, brain stem was more useful due to its lower variability compared with the previous study, presumably because of the longer half-life of  $^{18}\text{F}$  and its lower positron range than  $^{11}\text{C}$ .

## Conclusions

Here, we validated the specificity of [ $^{18}\text{F}$ ]SynVesT-1 to mouse SV2A *in vitro* using both homologous and an autoradiography-based binding assay. To our knowledge, this is the first study to report *in vitro* assessments of [ $^{18}\text{F}$ ]SynVesT-1 binding to mouse SV2A, which is an important validation step for future preclinical studies using mouse disease models investigating synaptic density dynamics following drug treatment or other interventions. We have developed a simplified quantification method for SV2A in APP/PS1 mice and wild type controls using [ $^{18}\text{F}$ ]SynVesT-1 and small animal PET, supporting further evaluations and validations of this tracer in other disease models. SUVR-1<sub>(BS)</sub> using data from a static PET scan from 30–60 min *p.i.* and brain stem as reference region provides reliable estimation of specific-binding ( $BP_{ND}$ ). Using this simplified



quantification method, [ $^{18}\text{F}$ ]SynVesT-1 is likely to have wide use in rodent model studies, since [ $^{18}\text{F}$ ]SynVesT-1 has been shown to have excellent imaging qualities across species including early human scans and will likely play an important role in both preclinical and clinical research. The application of this imaging and quantification method in the preclinical evaluation of therapeutic drugs will be reported in due date.

*Supplementary Information.* The online version contains supplementary material available at <https://doi.org/10.1007/s11307-020-01567-9>.

*Acknowledgments.* The authors would like to acknowledge the Yale PET Center staff for their expert technical assistance. The authors thank Ivailo Mihaylov and Anthony D'Abramo Jr for their assistance with autoradiography study.

**Funding.** This research was supported by National Institutes of Health (NIH) K01EB023312, R01AG058773, R01AG052560. Z.C. is an Archer Foundation Research Scientist.

#### Compliance with Ethical Standards

#### Conflict of Interest

The authors declare that they have no conflict of interest.

#### Ethical Approval

All procedures performed in studies involving animals were in accordance with ethical standards of the Yale University Institutional Animal Care and Use Committee.

#### References

- Bajjalieh SM, Frantz GD, Weimann JM, McConnell SK, Scheller RH (1994) Differential expression of synaptic vesicle protein 2 (SV2) isoforms. *J Neurosci* 14:5223–5235
- Cai Z, Li S, Matuskey D, Nabulsi N, Huang Y (2019) PET imaging of synaptic density: A new tool for investigation of neuropsychiatric diseases. *Neuroscience Letters* 691:44–50
- Holmes SE, Scheinost D, Finnema SJ, Naganawa M, Davis MT, DellaGioia N, Nabulsi N, Matuskey D, Angarita GA, Pietrzak RH, Duman RS, Sanacora G, Krystal JH, Carson RE, Esterlis I (2019) Lower synaptic density is associated with depression severity and network alterations. *Nat Commun* 10:1529
- Finnema SJ, Nabulsi NB, Eid T et al (2016) Imaging synaptic density in the living human brain. *Sci Transl Med* 8:348ra396
- Onwordi EC, Half EF, Whitehurst T, Mansur A, Cotel MC, Wells L, Creney H, Bonsall D, Rogdaki M, Shatalina E, Reis Marques T, Rabiner EA, Gunn RN, Natesan S, Vernon AC, Howes OD (2020) Synaptic density marker SV2A is reduced in schizophrenia patients and unaffected by antipsychotics in rats. *Nat Commun* 11:246
- Matuskey D, Tinaz S, Wilcox KC, Naganawa M, Toyonaga T, Dias M, Henry S, Pittman B, Ropchan J, Nabulsi N, Suridjan I, Comley RA, Huang Y, Finnema SJ, Carson RE (2020) Synaptic changes in Parkinson disease assessed with in vivo imaging. *Ann Neurol* 87:329–338
- Nabulsi NB, Mercier J, Holden D, Carre S, Najafzadeh S, Vandergoten MC, Lin SF, Deo A, Price N, Wood M, Lara-Jaime T, Montel F, Laruelle M, Carson RE, Hannestad J, Huang Y (2016) Synthesis and preclinical evaluation of  $^{11}\text{C}$ -UCB-J as a PET tracer for imaging the synaptic vesicle glycoprotein 2A in the brain. *J Nucl Med* 57:777–784
- Mecca AP, Chen M-K, O'Dell RS, Naganawa M, Toyonaga T, Godek TA, Harris JE, Bartlett HH, Zhao W, Nabulsi NB, Wyk BCV, Varma P, Arnsten AFT, Huang Y, Carson RE, Dyck CH (2020) In vivo measurement of widespread synaptic loss in Alzheimer's disease with SV2A PET. *Alzheimer's & Dementia* 16:974–982
- Chen M-K, Mecca AP, Naganawa M, Finnema SJ, Toyonaga T, Lin SF, Najafzadeh S, Ropchan J, Lu Y, McDonald JW, Michalak HR, Nabulsi NB, Arnsten AFT, Huang Y, Carson RE, van Dyck CH (2018) Assessing synaptic density in Alzheimer disease with synaptic vesicle glycoprotein 2A positron emission tomographic imaging. *JAMA Neurology* 75:1215–1224
- Toyonaga T, Smith LM, Finnema SJ, Gallezot JD, Naganawa M, Bini J, Mulnix T, Cai Z, Ropchan J, Huang Y, Strittmatter SM, Carson RE (2019) In vivo synaptic density imaging with  $^{11}\text{C}$ -UCB-J detects treatment effects of saracatinib in a mouse model of Alzheimer disease. *J Nucl Med* 60:1780–1786
- Cai Z, Li S, Zhang W, Pracitto R, Wu X, Baum E, Finnema SJ, Holden D, Toyonaga T, Lin SF, Lindemann M, Shiralil A, Labaree DC, Ropchan J, Nabulsi N, Carson RE, Huang Y (2020) Synthesis and preclinical evaluation of an ( $^{18}\text{F}$ )-labeled synaptic vesicle glycoprotein 2A PET imaging probe: [ $^{18}\text{F}$ ]SynVesT-2. *ACS Chem Neurosci* 11:592–603
- Li S, Cai Z, Wu X, Holden D, Pracitto R, Kapinos M, Gao H, Labaree D, Nabulsi N, Carson RE, Huang Y (2019) Synthesis and in vivo evaluation of a novel PET radiotracer for imaging of synaptic vesicle glycoprotein 2A (SV2A) in nonhuman primates. *ACS Chem Neurosci* 10:1544–1554
- Naganawa M, Li S, Nabulsi NB, Henry S, Zheng MQ, Pracitto R, Cai Z, Gao H, Kapinos M, Labaree D, Matuskey D, Huang Y, Carson RE (2020) First-in-human evaluation of  $^{18}\text{F}$ -SynVesT-1, a novel radioligand for PET imaging of synaptic vesicle protein 2A. *J Nucl Med*. <https://doi.org/10.2967/jnumed.120.249144>
- Jankowsky JL, Fadale DJ, Anderson J et al (2003) Mutant presenilins specifically elevate the levels of the 42 residue  $\beta$ -amyloid peptide in vivo: evidence for augmentation of a 42-specific  $\gamma$  secretase. *Human Molecular Genetics* 13:159–170
- Gimbel DA, Nygaard HB, Coffey EE, Gunther EC, Lauren J, Gimbel ZA, Strittmatter SM (2010) Memory impairment in transgenic Alzheimer mice requires cellular prion protein. *J Neurosci* 30:6367–6374
- Um JW, Nygaard HB, Heiss JK, Kostylev MA, Stagi M, Vortmeyer A, Wisniewski T, Gunther EC, Strittmatter SM (2012) Alzheimer amyloid- $\beta$  oligomer bound to post-synaptic prion protein activates Fyn to impair neurons. *Nature Neuroscience* 15:1227–1235
- Um Ji W, Kaufman Adam C, Kostylev M et al (2013) Metabotropic glutamate receptor 5 is a coreceptor for Alzheimer A $\beta$  oligomer bound to cellular prion protein. *Neuron* 80:531
- Lammertsma AA, Hume SP (1996) Simplified reference tissue model for PET receptor studies. *Neuroimage* 4:153–158
- Logan J, Fowler JS, Volkow ND, Wang GJ, Ding YS, Alexoff DL (1996) Distribution volume ratios without blood sampling from graphical analysis of PET data. *J Cereb Blood Flow Metab* 16:834–840
- Kaminski RM, Gillard M, Leclercq K, Hanon E, Lorent G, Dasselme D, Matagne A, Klitgaard H (2009) Proepileptic phenotype of SV2A-deficient mice is associated with reduced anticonvulsant efficacy of levetiracetam. *Epilepsia* 50:1729–1740
- Gillard M, Fuks B, Leclercq K, Matagne A (2011) Binding characteristics of brivaracetam, a selective, high affinity SV2A ligand in rat, mouse and human brain: relationship to anti-convulsant properties. *Eur J Pharmacol* 664:36–44
- Patel S, Knight A, Krause S et al (2019) Preclinical in vitro and in vivo characterization of synaptic vesicle 2A-Targeting compounds amenable to F-18 labeling as potential pet radioligands for imaging of synapse integrity. *Mol Imaging Biol*. 22:832–841
- Lynch BA, Lambeng N, Nocka K, Kensel-Hammes P, Bajjalieh SM, Matagne A, Fuks B (2004) The synaptic vesicle protein SV2A is the binding site for the antiepileptic drug levetiracetam. *Proc Natl Acad Sci USA* 101:9861–9866
- Mercier J, Archen L, Bollu V, Carré S, Evrard Y, Jnoff E, Kenda B, Lallemand B, Michel P, Montel F, Moureau F, Price N, Quesnel Y, Sauvage X, Valade A, Provins L (2014) Discovery of heterocyclic nonacetamide synaptic vesicle protein 2A (SV2A) ligands with single-digit nanomolar potency: opening avenues towards the first SV2A positron emission tomography (PET) ligands. *ChemMedChem* 9:693–698

25. Estrada S, Lubberink M, Thibblin A, Sprycha M, Buchanan T, Mestdagh N, Kenda B, Mercier J, Provins L, Gillard M, Tytgat D, Antoni G (2016) [<sup>11</sup>C]UCB-A, a novel PET tracer for synaptic vesicle protein 2 A. *Nucl Med Biol* 43:325–332
26. Warnock GI, Aerts J, Bahri MA, Bretin F, Lemaire C, Giacomelli F, Mievis F, Mestdagh N, Buchanan T, Valade A, Mercier J, Wood M, Gillard M, Seret A, Luxen A, Salmon E, Plenevaux A (2014) Evaluation of <sup>18</sup>F-UCB-H as a novel PET tracer for synaptic vesicle protein 2A in the brain. *J Nucl Med* 55:1336–1341
27. Hong S, Beja-Glasser VF, Nfonoyim BM, Frouin A, Li S, Ramakrishnan S, Merry KM, Shi Q, Rosenthal A, Barres BA, Lemere CA, Selkoe DJ, Stevens B (2016) Complement and microglia mediate early synapse loss in Alzheimer mouse models. *Science* 352:712–716
28. Pozueta J, Lefort R, Shelanski ML (2013) Synaptic changes in Alzheimer's disease and its models. *Neuroscience* 251:51–65
29. Bertoglio D, Verhaeghe J, Miranda A, et al. (2019) Validation and noninvasive kinetic modeling of [<sup>11</sup>C]UCB-J PET imaging in mice. *J Cereb Blood Flow Metab* 0:271678X19864081.
30. Naganawa M, Gallezot J-D, Finnema S, Matuskey D, Mecca AP, Nabulsi NB, Labaree D, Ropchan J, Malison RT, D'Souza DC, Esterlis I, Detyniecki K, van Dyck CH, Huang Y, Carson RE (2020) Simplified quantification of <sup>11</sup>C-UCB-J PET evaluated in a large human cohort. *J Nucl Med*. <https://doi.org/10.2967/jnumed.120.243949>
31. Cai Z, Li S, Zhang W et al (2020) Synthesis and preclinical evaluation of an <sup>18</sup>F-labeled synaptic vesicle glycoprotein 2A PET imaging probe: [<sup>18</sup>F]SynVesT-2. *ACS Chem Neurosci* 11(4):592–603
32. Li S, Cai Z, Zhang W, Holden D, Lin SF, Finnema SJ, Shirali A, Ropchan J, Carre S, Mercier J, Carson RE, Nabulsi N, Huang Y (2019) Synthesis and in vivo evaluation of [<sup>18</sup>F]UCB-J for PET imaging of synaptic vesicle glycoprotein 2A (SV2A). *Eur J Nucl Med Mol Imaging* 46:1952–1965
33. Rossano S, Toyonaga T, Finnema SJ et al (2019) Assessment of a white matter reference region for (<sup>11</sup>C)-UCB-J PET quantification. *J Cereb Blood Flow Metab* 40:1890–1901

**Publisher's Note** Springer Nature remains neutral with regard to jurisdictional claims in published maps and institutional affiliations.